Journal of Alloys and Compounds 478 (2009) 586–589

Contents lists available at ScienceDirect

Journal of Alloys and Compounds

journal homepage: www.elsevier.com/locate/jallcom

Mixed-phase TiO_2 nanoparticles preparation using sol–gel method

S. Mahshid [a], M. Askari [a], M. Sasani Ghamsari [b,*], N. Afshar [c], S. Lahuti [c]

[a] Department of Material Science & Eng., Sharif University of Technology, 11365-9466 Tehran, Iran
[b] Solid State Lasers Research Group, Laser & Optics Research School, NSTRI, North Karegar, 11365-8486 Tehran, Iran
[c] Materials Characterization Lab., Materials Research School, NSTRI, Karaj, Iran

ARTICLE INFO

Article history:
Received 18 September 2008
Received in revised form
18 November 2008
Accepted 21 November 2008
Available online 30 November 2008

Keywords:
TiO_2 Nanostructures
Sol–gel chemistry
Phase transactions

ABSTRACT

Biphase TiO_2 nanoparticles have been prepared by sol–gel method. Water/titanium molar ratio (r) has been used to control the hydrolysis and condensation of titanium isopropoxide in solution producing titanium oxide with two different polymorphs. The influence of crystallite size and morphology of prepared TiO_2 on the phase transformation of the resultant materials has been investigated. Synthesized powders were characterized by X-ray diffraction, scanning electron microscopy (SEM) and transmission electron microscopy (TEM). Different trends can be observed in the phase transformation and particle growth of the prepared titanium oxide nanomaterial. It was concluded that, the rate of particle growth and the final particle size as well as phase transformation were a function of molar ratios (r). The percentage of rutile in the final material was 23%.

1. Introduction

In recent years, applications of semiconductor metal oxide nanoparticles are getting more extensive covering different fields such as optoelectronics, catalysis, medicine, and sensor devices. Besides, the quantum size effects, the parameters such as structure; size, shape, and elemental composition are considered to be highly important for promising applications of the nanomaterials. Among the metal oxide nanostructures, TiO_2 has extensively been explored for several technological applications such as catalysis, gas sensing, cancer treatment, dye-sensitized solar cells and photonic crystal [1–3]. Such applications of titania have been found to depend strongly on the crystalline structure, morphology, and particle size [4,5]. On the other hand, the theoretical study and experimental results have shown that the photocatalytic and photovoltaic properties of TiO_2 nanoparticles with two different polymorphic phases (anatase and rutile) are better than pure anatase titanium nanoparticles [6–12]. Mixed-phase TiO_2 material has recently been fabricated by chemical and physical methods, including a sol–gel, hydrothermal, solvothermal, and reactive DC magnetron sputtering method, and has demonstrated excellent photocatalytic activities [13–15]. As usual, the preparation of titanium nanomaterial with two different polymorphs by sol–gel method needs to crystallize the as-prepared titanium hydroxide at high temperature ($\geq$700 °C). This heat treatment leads to change in the crystallite size as well as morphology of the sol–gel derived titanium oxide [16,17]. Therefore, the preparation of mixed phase titanium oxide at lower temperature will be useful both in saving energy and in getting better properties. There is no study, known to us, which attempted to prepare TiO_2 biphase by sol–gel method at lower temperature ($\leq$500 °C). In this approach, we have tried to control the phase transformation of TiO_2 nanopowders and to obtain mixed phase of titanium oxide at lower temperature. In addition, the effects of different parameters such as crystallite size and morphology on the phase transformation of prepared TiO_2 nanoparticles have been discussed.

2. Experimental

The preparation of TiO_2 nanoparticles by sol–gel method has been carried out in several steps and it needs to mix two different solutions. These two solutions are called as precursor and hydrolysis solutions. In our procedure, the precursor solution is a mixture of 5 ml titanium isopropoxide, TTIP (97%, and supplied by Aldrich Chemical) and 15 ml 2-propanol (99%, supplied by Merck). The hydrolysis solution is a mixture of distilled water and 2-propanol. In order to control the sol–gel reactions (hydrolysis and condensation), different molar ratios of water–isopropyl alcohol have been used as hydrolysis solutions (Table 1) [18]. The pH of hydrolysis solution must be adjusted by HNO_3 acid. Here, we have to emphasize that the preparation of these two solutions is very important and the final results depend highly on the preparation conditions of these starting materials [19]. The gel preparation process was started when the precursor and hydrolysis solutions were mixed together under vigorous stirring at room temperature. After mixing for several minutes, the stirring rate was reduced in order to minimize coagulation of the titanium oxide particles during the sol–gel reactions. The prepared titanium hydroxide was then washed with ethanol, dried for several hours at 100 °C, and annealed at different temperatures for 2 h. Powder X-ray diffraction (Philips PW 1800) instrument was used for crystal phase identification and estimation of the average crystallite size. The (1 0 1) peak of anatase and (1 1 0) peak of rutile have been considered for crystallite size estimation respectively. In order to determine the particle size and morphology of nanopowder, the calcined samples were dispersed in distilled water

* Corresponding author. Tel.: +98 21 88008592; fax: +98 21 88009188.
E-mail address: msghamsari@yahoo.com (M. Sasani Ghamsari).

0925-8388/$ – see front matter © 2008 Elsevier B.V. All rights reserved.
doi:10.1016/j.jallcom.2008.11.094

Table 1
Solvents concentration in precursor and hydrolysis solution.

Sample	Precursor solution		Hydrolysis solution		Final volume (ml)
	TTIP (ml)	2-Propanol (ml)	Distilled water (ml)	2-Propanol (ml)	
A1	5	15	100	150	270
A2	5	15	25	225	270
A3	5	15	5	245	270
A4	5	15	25	75	120
A5	5	15	5	95	120
A6	5	15	2.5	97.5	120

Table 2
Visual observation of the sol to gel conversion after mixing the precursor and hydrolysis solutions.

Sample	$[H_2O]/[Ti^{+4}]$	After mixing	Sol–gel conversion
A1	265	White suspension with large precipitates	No gel
A2	66	White homogenous suspension with small precipitates	Semi-liked gel structure after 3 h
A3	13	Light blue transparent sol	Complete gel after 10–15 min
A4	66	White suspension	Semi-liked and watery gel structure after several hours
A5	13	Blue–white, homogenous suspension	Semi-liked and watery gel structure after 3–4 h
A6	6.6	Light blue transparent	Sol perfect gel after 10–15 min

and sonicated ultrasonically by using a Cole-Parmer 8851 apparatus, to separate out individual particles. The size and morphology of the powder were then observed on Philips XL 30 scanning electron microscope (SEM) and Philips 200 transmission electron microscope (TEM).

3. Results and discussion

The careful observation of the sol to gel conversion was carried out for all the samples and the results gathered in Table 2. X-ray diffraction patterns of the calcined samples at 200 °C showed that the powders are mostly amorphous and contain very low crystallized TiO_2. Heat treatment of prepared powders at 400 °C causes the crystallization of the anatase polymorph. Fig. 1 shows the X-ray diffraction patterns of the annealed samples at 400 °C for almost 2 h. The average crystallite size has easily been determined by Debby–Scherrer formula considering (1 0 1) anatase peak and listed in Table 3. Apart from this technique and in order to confirm the calculated crystallite size from Scherrer formula, TEM images of sample A5 have been taken for comparison. This image is illustrated in Fig. 2 and shows that the particle size is in good agreement to the estimated sizes by Scherrer's formula. X-ray diffraction patterns of heat treated samples at 500 °C have been shown in Fig. 3. The study of experimental results reveals that different phenomena can be observed in the phase transformation and grain growth of calcined samples.

From phase transformation and particle growth points of view, we have found different results. Two phenomena have been observed when annealing temperature increases to 550 °C. One is the rutile to anatase transformation in samples A5 and A6. Another is the change of average crystallite size during heat treatment. Nevertheless, the crystallite size of samples A3 (35 nm) and A5 (42 nm) are almost near each other, one can also find that there are other parameters which affect the temperature of anatase to rutile phase transformation. This is not in agreement with the reported results by Ding et al. [20] and Zhang et al. [21,22] who had concluded that anatase crystallite size was the main factor lowering A–R transformation temperature. As it has been reported in Ref. [23,24], the phase transformation of anatase to rutile is a surface phenomena. So this means that the transformation is associated with nucleation on the surface of particles. It is believed that the difference between chemical potential of primary and final phases is the most likely factor which is responsible for activation energy of phase transformation. Nanoparticles with small crystallite size have less thermal stability. In the case of solid particles, the total free energy is determined by volume energy G_V, surface energy G_S and surface stress induced energy G_f. In comparison with bulk of materials, the last two terms are very large in nanoparticles and so they could not be ignored. The surface energy is increased by the construction of new surface which is due to nanoparticles formation. The Gibbs free energy of phase transformation for anatase nanoparticles is as follow [24]:

$$\begin{aligned}\Delta G_{A\to R} &= \Delta G_{V,R}(T) - \Delta G_{V,A}(T) + (A_R\gamma_R - A_A\gamma_A) \\ &\quad + (\Delta P_R V_R - \Delta P_A V_A) \\ &= \Delta G_{V,R}(T) - \Delta G_{V,A}(T) + \left(\frac{3M\gamma_R}{\rho_R r_R} - \frac{3M\gamma_A}{\rho_A r_A}\right) \\ &\quad + \left(\frac{2Mf_R}{\rho_R r_R} - \frac{3Mf_A}{\rho_A r_A}\right) \end{aligned} \quad (1)$$

where γ is the surface free energy, A is the surface area, r is the particle radius, ΔP is the surface stress, V is the molar volume, M

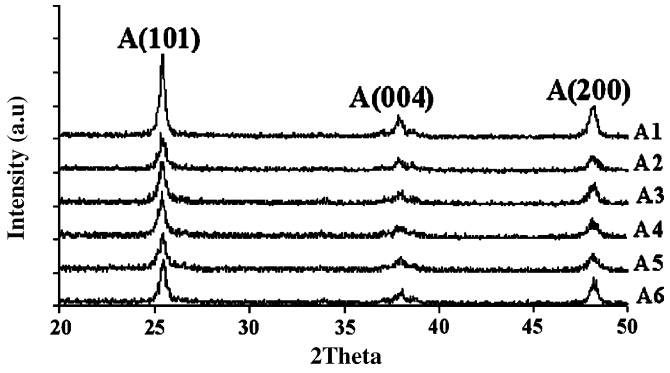

Fig. 1. X-ray diffraction pattern of different calcined samples at 400 °C for 2 h.

Table 3
Average crystallite size of calcined samples at different temperature.

Sample	Mean size (nm)		
	At 400 °C	At 550 °C	%Transformation
A1	106 (A)	27 (A)	–
A2	35 (A)	49 (A)	–
A3	35 (A)	47 (A)	–
A4	53 (A)	85 (A)	–
A5	42 (A)	85 (A), 107 (R)	23
A6	30 (A)	53 (A), 85 (R)	22.5

(A): anatase; (R): rutile.

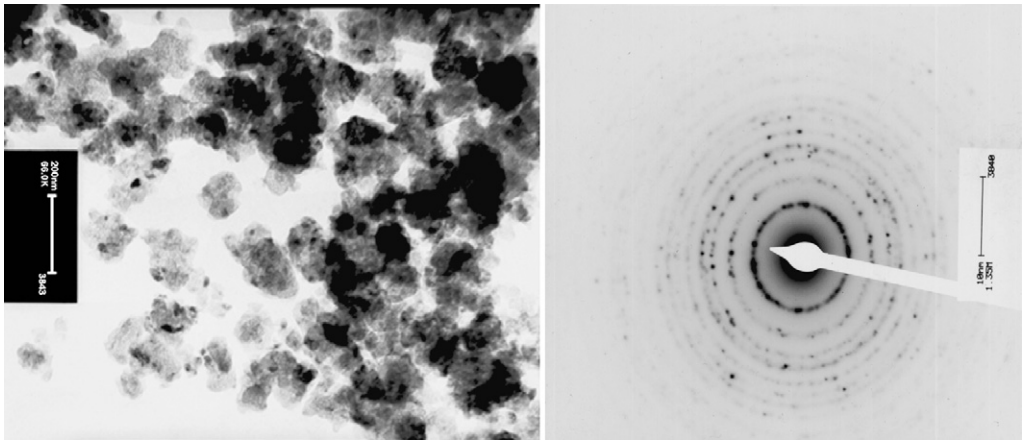

Fig. 2. TEM photograph and diffraction pattern of sample A5 that have calcined at 400 °C for 2 h.

is the molecular weight, ρ is the phase density and f is the related excess pressure with a value of $2fr^{-1}$.

Only a large negative $\Delta G_{A\rightarrow R}$ is an adequate driving force for anatase to rutile transformation. According to Eq. (1), anatase energies from both surface and stress have negative contribution to the total energy difference between rutile and anatase. Thus, the higher surface energy and surface stress energy have more contribution to the non-equilibrium transition from anatase to rutile. Particles with smaller sizes have large surface areas and higher surface energy. Therefore, in anatase with smaller particle size it is easier to start the phase transformation at lower temperature than in the large particles under similar condition. The higher negative $\Delta G_{A\rightarrow R}$ value corresponds to the lower activation energy which is needed for anatase to rutile transition [24]. Activation energy of 418–753 kJ/mol was reported for millimeter-sized anatase single crystals in the temperature range 900–950 °C, while a much lower value of 166 ± 1 kJ/mol was found for nanocrystalline anatase prepared by the sol–gel method in the temperature range 465–525 °C [25].

According to above argument, the decreasing of the surface area leads to increase the activation energy and avoids the phase transformation at low temperature. Thus, in the particles with the same size and different surface area different behavior in phase transformation must be observed. Study of samples by scanning electron microscope has shown that the surface area of sample A5 with larger particles size is lower than sample A3 and the lower agglomeration has been found. In other words, in the sample A3 with smaller particle size more agglomeration has been occurred which intends to less phase transformation (Fig. 4). Therefore, we can conclude that the shape and surface morphology of heat treated nanopowders have a critical role in the phase transformation of anatase to rutile.

If the particle size is considered to be the only predominant factor affecting transition kinetics, we expect that the lower grain size of powders would accelerate phase transformation. There is another phenomenon that can be observed in the particle growth behavior of sample A1. The sample A1 has shown different grain growth behavior. After heat treatment at 500 °C, the change in the crystallite size of sample A1 is different from other samples. One cannot find a simple trend in growth and final size of different samples. A general trend can be found, if we select the average crystallite size ratio of samples at 550 °C to 400 °C as criteria. This crystallite size ratio has been nominated as D_{550}/D_{400} and presented in Fig. 5. This figure shows that at a fixed concentration of TTIP in solution, D_{550}/D_{400} decreases as the molar ratio (r) value increases. In other words, anatase crystallite size of the powder with lower molar ratio (r) values tends to grow more rapidly when heated to higher temperatures. The final size of the crystallites is determined by the relative rate of particle growth. Elevation of temperature not only accelerates nucleation rate but also enhances particle growth. Depending on the primary particle size and agglomeration which has influence on the nucleation sites density, one of the nucleation or growth mechanisms will dominate in high temperature heat treatment. Therefore, it can be concluded that as the molar ratio

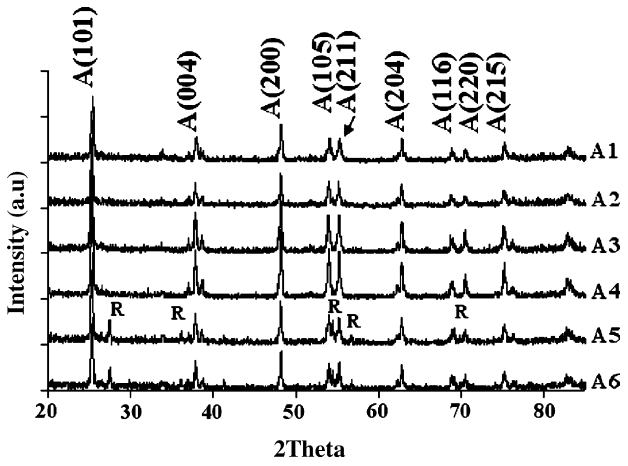

Fig. 3. X-ray diffraction pattern of different calcined samples at 550 °C for 2 h (A: anatase, R: rutile).

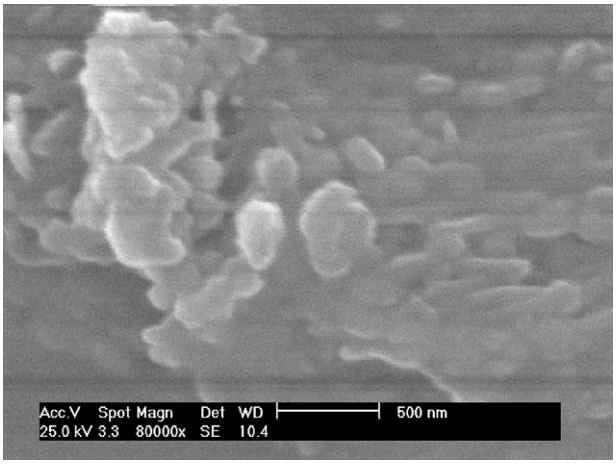

Fig. 4. SEM photograph of sample A3 calcined at 550 °C for 2 h.

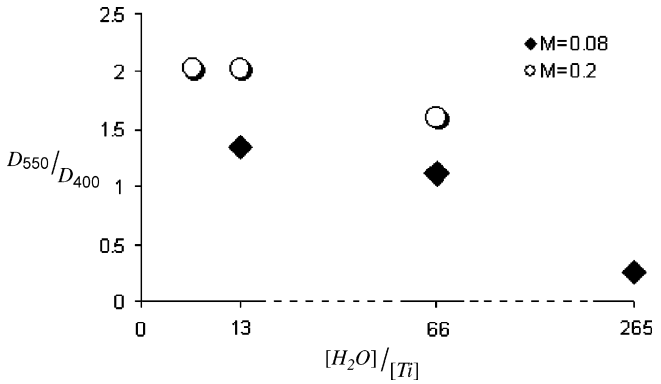

Fig. 5. The variation of the crystallite size ratio with respect to water–titanium molar ratio of the prepared samples and heated at 550 °C and 400 °C. The symbol M is molar concentration of Ti^{4+}.

(r) increases, the average crystallite size ratio of the calcined particles (D_{550}/D_{400}) will reduce which is due to the predominance of nucleation mechanism. On the other hand, at a fixed molar ratio (r), when the TTIP concentration in the sol increases the D_{550}/D_{400} will increase which indicates that the prepared crystallite from higher TTIP concentration solution tends to grow at higher temperature and grain growth is dominant phenomenon.

4. Conclusion

The results show that an increase in the water–titanium molar ratio causes an increase of average size of the formed crystallite. Different trends can be observed in the phase transformation and particle growth of the prepared titanium oxide nanomaterial. The shape and morphology of heat treated nanopowders have a critical role in the phase transformation of anatase to rutile. In the prepared powders with high water–titanium molar ratio, nucleation plays the main role in the formation rate of new crystallites, when the temperature rises from 400 °C to 550 °C. It is also found that grain growth is dominant mechanism for particle growth in the heat treated sample with low water–titanium molar ratio. It is concluded that the percentage of rutile polymorph in the heat treated powder can be controlled by water–titanium molar ratio.

References

[1] T. Thompson, J. Yates Jr., Chem. Rev. 106 (2006) 4428–4453.
[2] M. Pal, J. Garcya Serrano, P. Santiago, U. Pal, J. Phys. Chem. C 111 (2007) 96–102.
[3] S. Ito, T.N. Murakami, P. Comte, P. Liska, C. Grätzel, M.K. Nazeeruddin, M. Grätzel, Thin Solid Films 516 (2008) 4613–4619.
[4] H. Lin, C.P. Huang, W. Li, C. Ni, S. Ismat Shah, Y.-H. Tseng, Appl. Catal. B: Environ. 68 (2006) 1–11.
[5] B. Gao, Y. Ma, Y. Cao, J. Zhao, J. Yao, J. Solid State Chem. 179 (2006) 41–48.
[6] N.A. Deskins, S. Kerisit, K.M. Rosso, M. Dupuis, J. Phys. Chem. C 111 (2007) 9290–9298.
[7] D. Jiang, S. Zhang, H. Zhao, Environ. Sci. Technol. 41 (2007) 303–308.
[8] Q. Shen, K. Katayama, T. Sawada, M. Yamaguchi, Y. Kumagai, T. Toyoda, Chem. Phys. Lett. 419 (2006) 464–468.
[9] B. Sun, P. Smirniotis, Catal. Today 88 (2003) 49–59.
[10] I. Zumeta, R. Espinosa, J.A. Ayllon, X. Domenech, R. Rodriguez-Cclemente, E. Vigil, Solar Energy Mater. Solar Cell 76 (2003) 15–24.
[11] T. Kawahara, Y. Konishi, H. Tada, N. Tohge, J. Nishii, S. Ito, Angew. Chem. Int. Ed. 41 (2002) 2811–2813.
[12] J.H. Jho, D.H. Kim, S.-J. Kim, K.S. Lee, J. Alloys Compd. 459 (2008) 386–389.
[13] G. Li, S. Ciston, Z.V. Saponjic, L. Chen, N.M. Dimitrijevic, T. Rajh, K.A. Gray, J. Catal. 253 (2008) 105–110.
[14] M. Kanna, S. Wongnawa, Mater. Chem. Phys. 110 (2008) 166–175.
[15] H. Choi, Y.J. Kim, R.S. Varma, D.D. Dionysiou, Chem. Mater. 18 (2006) 5377–5384.
[16] N. Wetchakun, S. Phanichphant, Curr. Appl. Phys. 8 (2008) 343–346.
[17] H.-I. Hsiang, S.-C. Lin, Ceram. Int. 34 (2008) 557–561.
[18] S. Mahshid, M. Askari, M. Sasani Ghamsari, 1st International Congress on Nanoscience and Nanotechnology, University of Tehran, Iran, 2006.
[19] S. Mahshid, M. Askari, M. Sasani Ghamsari, J. Mater. Process. Technol. 189 (2007) 296–300.
[20] X.Z. Ding, X.H. Liu, J. Alloys Compd. 248 (1997) 143–145.
[21] H. Zhang, J.F. Banfield, J. Mater. Chem. 8 (1998) 2073–2076.
[22] H. Zhang, J.F. Banfield, J. Phys. Chem. B 104 (2000) 3481–3487.
[23] C.M. Ronconi, C. Ribeiro, L.O.S. Bulhoes, E.C. Pereira, J. Alloys Compd. 466 (2008) 435–438.
[24] W. Li, C. Ni, H. Lin, C.P. Huang, S. Ismat Shah, J. Appl. Phys. 96 (2004) 6663–6668.
[25] J.G. Li, T. Ishigaki, Acta Mater. 52 (2004) 5143–5150.